Celal Bayar University Journal of Science

Recent Advancements in Computational Approaches for Tailoring Toll-like Receptors and Antimicrobial Peptides Against Candida Infections

Mesude Biçer[1*], Onur Serçinoğlu[2], Tuba Okur[2]

[1]Department of Bioengineering, Faculty of Life and Natural Sciences, Abdullah Gul University, Kayseri 38080, Türkiye
[2]Department of Bioengineering, Faculty of Engineering, Gebze Technical University, Gebze, Kocaeli, 41400, Türkiye
* mesude.bicer@agu.edu.tr
* Orcid: 0000-0001-7089-5661

Received: November 30, 2024
Accepted: March 8, 2025
DOI: 10.18466/cbayarfbe.1593863

Abstract

Despite the considerable pathogenic impact of Candida albicans in human health, the gap in understanding the cellular recognition mechanisms and subsequent host defence activation remain insufficiently understood. Recent insights underscore the pivotal role of Toll-like receptors (TLRs) in organising innate immune responses against pathogens. Notably, empirical investigations over recent years have underscored TLRs as paramount pattern-recognition receptors in mammals. TLR2, for examples, exhibits affinity for peptidoglycans, lipoarabinomannan, and bacterial lipoproteins, while TLR4 implicated in detecting lipopolysaccharide (LPS) and lipo-teichoic acid. Similarly, TLR5 recognizes flagellin, and TLR9 is associated with bacterial DNA recognition. The initial identification of Toll in Drosophila as a regulator of antifungal mechanisms suggests the potential involvement of TLRs in mammalian antifungal defence. However, scant attention has been devoted to delineating the role of TLRs in combating fungal pathogens in humans, despite the evolutionary link between Toll in Drosophila and antifungal mechanisms, suggesting a plausible involvement of TLRs in mammalian antifungal defense. Notably, evidence implicates TLR4, but not TLR2, in inducing proinflammatory cytokines in response to Aspergillus fumigatus, while its role is purported to mediate intracellular signaling, albeit not TNF production, after stimulation of cells with *Cryptococcus neoformans*. However, insights into TLR activation rules have enabled the examination of antimicrobial peptide (AMP) interactions with TLRs, facilitating predictions regarding the immunomodulatory capacities of diverse molecules. Despite these advancements, the specific role of TLRs in recognizing *Candida albicans*, a prominent human pathogen, remains elusive, warranting further investigation. This computational approach synthesizes recent findings elucidating the interactions between AMPs and TLRs, delineating the structural determinants governing TLR activation, thus enabling predictive insights into the immunomodulatory potential of diverse molecular entities.

Keywords: Toll-like receptors, antimicrobial peptide, candida infections, computational approaches, protein-protein docking, molecular dynamics simulation, tissue engineering

1. Introduction

Fungal infections represent a global health concern with a rapid climb in incidence observed over the past three decades, affecting both immunocompromised patients and those considered healthy individuals [1, 2]. The prevalence of superficial fungal infections is estimated to surpass 1 billion cases annually, with a tendency toward underreporting and escalating incidence [2]. Among fungal strains, *Candida* strains, particularly *Candida albicans*, exhibit significant clinical relevance, ranking as the fourth cause of nosocomial bloodstream infections in numerous European countries and the United States [3]. *Candida albicans* remains a predominant etiological agent across mucosal and systemic infections, leading substantially to morbidity and mortality [4]. The treatment landscape for serious fungal infections primarily revolves around polyene antifungal drugs (amphotericin B) and its lipid formulations, azoles including fluconazole, itraconazole, voriconazole, posaconazole, and echinocandins including caspofungin, micafungin, and anidulafungin [5]. Although amphotericin B was previously regarded as the gold standard for invasive fungal infections, its nephrotoxicity

and related renal failure have resulted in its restricted utilization, with lipid formulations emerging as alternatives albeit with higher costs [6]. Fluconazole have prized for its high oral absorption rate and independence from gastric pH [7], and finds preferential approaches in candida infections due to its urinary concentration, facilitating the management of Candida spp. urinary infections [8]. Echinocandins, the novel class of antifungals, represent efficacy in invasive infections and are recommended as initial therapy based on compelling evidence interacting them with reduced mortality from patient-level analysis of randomized trial data [9, 10]. Contrarily, itraconazole's limited bioavailability and inclination for adverse effects and drug interactions restrict its clinical utility [11].

The surge in candidemia incidence is associated with some factors such as the increased invasive procedures, the heightened susceptibility within risk populations, the prolonged medical device usage and randomly use of broad-spectrum antibiotics and chemotherapeutic formulations [12]. Despite advancements in antifungal pharmacology, common invasive fungal infections continue to bear high mortality rates, underscoring the urgent need for novel antifungal agents targeting diverse fungal vulnerabilities [13]. Antimicrobial peptides (AMPs) exhibit a promising avenue in this pursuit, with research indicating their potential in attenuating pathogen virulence, particularly in inhibiting biofilm formation. The Antimicrobial Peptide Database currently catalogues a significant number of AMPs, with ongoing interest in their design and development toward combating drug-resistant infections and modulating immune responses [14]. AMPs are widely found in a variety of organisms such as bacteria, archaea, protists, fungi, plants, amphibians, insects, fish and mammals. AMPs, a significant component of innate immunity, are produced in areas of the body which are most vulnerable to pathogen invasion. As of January 2024, the Antimicrobial Peptide Database documents a vast array of peptides, including 3146 natural antimicrobial peptides and those with 1399 antifungal peptides and 144 human host defense properties, signaling the burgeoning interest in AMPs as therapeutic candidates. The data was accessed on 2 April 2024 from https://aps.unmc.edu/.

With the resurgence of drug-resistant infections, there is renewed emphasis on designing and developing AMPs with potent, selective activity and favorable immunomodulatory profiles [15, 16]. Utilizing an innovative amalgamation of techniques spanning chemistry, computational biology, and immune activation experiments, a novel physical approach for AMP-induced immunomodulation via Toll-like receptors (TLRs) is described. Current research focuses on distinguishing between agonistic and antagonistic roles of TLR-targeting agents and their tailored application in treating distinct diseases [17]. TLR agonists are employed to enhance innate immune responses for addressing various disorders such as cancers, chronic infections, and asthma, whereas TLR antagonists are responsible for managing inflammatory conditions like sepsis, chronic pulmonary and cardiovascular diseases, and autoimmune diseases [18, 19]. Recent studies have extensively explored the structural and ligand recognition aspects of Toll-like receptors, often utilizing computational methodologies for their analysis [20, 21]. The increasing incorporation of computational tools has led to a deeper comprehension of the complex interaction between TLRs and AMPs. Thus, the body of literature underscores the dual role of AMPs in triggering both pro-inflammatory and anti-inflammatory immune responses, contingent upon biological context of TLRs.

2. Materials and Methods

2.1. Data Collection/ or/ Retrieval and Prediction of Antimicrobial Peptides and Toll-like Receptors

Within the framework of the study, eight AMPs and five receptor TLR proteins were investigated. If the 3D structure of the studied AMP was not available at Protein Data Bank, 3D structures of TLR proteins, as predicted by AlphaFold 2, were retrieved from Uniprot (https://www.uniprot.org/) database [22]. Only extracellular domains of TLRs were used. TLRs whose structures were retrieved from the Uniprot are as follows: TLR2 (Uniprot entry ID: O60603), TLR3 (entry ID: O15455), TLR4 (entry ID: O00206), TLR8 (entry ID: Q9NR97), TLR9 (entry ID: Q9NR96). Structures of five AMPs were retrieved from protein databank (https://www.rcsb.org/) in pdb format [23]. The AMPs and their PDB IDs are as follows: betadefensin1 (PDB ID: 1IJV), betadefensin2 (PDB ID: 1FD3), betadefensin3 (PDB ID: 1KJ6), LL-37 (PDB ID: 2K6O). Structures of beta defensin 4, psoriasin, CGA-N46 and histatin 5 peptides were predicted using ColabFold-v.1.5.5 (https://github.com/sokrypton/ColabFold) [24].

2.2. Protein - Protein Docking and SASA Calculation

TLR proteins and peptides were docked onto each other using ClusPro (https://cluspro.org) protein-protein docking server [25]. All possible binding positions were evaluated visually to identify reasonable binding poses (i.e. between the AMP and the ligand binding interface of TLR). Changes in Solvent accessible solvent area (SASA) (Δ_{SASA}) values between unbound and bound complexes were calculated. Complexes showing the highest change were selected for Molecular Dynamics (MD) simulation study. SASA calculations were performed using PyMOL. Changes in SASA were calculated using the following equation (1).

$$\Delta_{SASA} = SASA_{Complex} - (SASA_{Peptide} + SASA_{Protein}) \quad (1)$$

2.3. Molecular Dynamics (MD) Simulations

AMP-TLR docked complexes were used as starting structures in MD simulations. Final structures were prepared using CHARMM-GUI web server for MD simulations [26, 27]. The systems include 0.15M K+ and Cl- ions. TIP3 was used as the water model. The systems were solvated with a 10.0 Å padding distance from each boundary in a box to create reasonable conditions for periodic boundaries. CHARMM36 force field was used in simulations [28], which were conducted using gromacs 2020 [29]. Each simulation was conducted for 100ns three times. Prior to each simulation, the prepared system was minimized with 5000 (10 ps) steps and equilibrated with 125000 (250ps) steps. The systems were simulated at 310 K, using a 2-fs time step. Visual Molecular Dynamics (VMD) was used to visualize trajectories [30]. Total simulation time was 2.4 microseconds (μs) for 24 systems. Each system was prepared for simulation using CHARMM-GUI webserver [26, 27].

2.4. Root Mean Square Deviation (RMSD) and Root Mean Square Fluctuation (RMSF) calculations

Root Mean Square Deviation (RMSD) and Root Mean Square Fluctuation (RMSF) calculations of three simulation repeats for each simulation complex were performed using ProDy [31]. RMSD time profiles were computed by superposing alpha-carbon coordinates onto the starting conformation. RMSF calculations were also similarly performed based on alpha-carbon coordinates, after selecting the equilibrated portions of trajectories (i.e. between 20 and 100 ns, identified based on the RMSD time profiles), and superposing the conformations in these portions onto the average conformation. Standard deviations were calculated for all simulations and shown in the graph.

2.5. Molecular Mechanics/Poisson-Boltzmann Surface Area (MM/PBSA) calculations

Molecular Mechanics/Poisson-Boltzmann Surface Area (MM/PBSA) calculations were performed to estimate the binding free energies (FEB) of the simulated AMP-TLR systems [32]. The analysis was conducted using 100 frames extracted from the equilibrated portions of the molecular dynamics (MD) simulation trajectories. gmx_MMPBSA was used to perform MM/PBSA calculations [33].

3. Results and Discussion

3.1. Data Collection/ or/ Retrieval and Prediction of Antimicrobial Peptides and Toll-like Receptors

The AMPs studies include beta defensin 1, beta defensin 2, beta defensin 3, beta defensin 4, CGA-N46, psoriasin, LL-37 and histatin 5. Potential interactions between these AMPs and five TLR receptors, namely TLR2, TLR3, TLR4, TLR8 and TLR9, were investigated. The selected TLR receptor proteins are not found in the Protein Data Bank as full structures, including the N-terminal domain (ectodomain responsible for ligand recognition), C-terminal domain (endodomain, cytoplasmic part of the protein responsible for signal transduction inside the cell), and finally the transmembrane part of the structure with helical structure [34]. During the AMPs recognition processes, ectodomain of TLRs plays a vital role [35]. Therefore, ectodomains of TLR Alphafold2-predicted structures were used in further modeling studies.

3.2. Protein - Protein Docking and SASA Calculation

Interaction of the AMPs and TLRs were evaluated [36]. For this purpose, a protein-protein rigid docking server, Cluspro, was used. Waters, ions and other heteroatoms were removed from the structure. In the experimental structures. Only single chains were used in docking simulations. All AMPs were found to dock onto surfaces of all five TLRs. In total, 40 protein-protein docking studies were performed. All results were visualized using PyMOL, and only results that yielded a reasonable interaction mode between the AMP and TLR were taken into consideration [37]. For each docked pairs, 10 out of 40 docking results were evaluated to choose best complex. The evaluation was based on calculation of changes in Solvent Accessible Surface Area (SASA) upon binding of AMPs to the TLRs [38]. In total, 400 docked complexes were evaluated. Only the docked complex showing the lowest SASA value was chosen for each AMP-TLR pair. Then, best AMP-TLR complex was chosen for each peptide by calculating Δ_{SASA} values (**Table 1**) using PyMOL. Failure to bury a significant surface area on the TLR, and thus relatively high delta-SASA values may indicate relatively instable systems [39] [40]. Therefore, docked complexes that showed lowest Δ_{SASA} value between each AMP and TLR were chosen as a starting file for further MD simulation studies. (**Figure1**). These pairs are highlighted in Table 1. It can be seen that the AMPs showed the most favorable interactions, in terms of buried SASA amounts, with either TLR8 and TLR9.

Celal Bayar University Journal of Science
Volume 21, Issue 3, 2025, p 1-9
Doi: 10.18466/cbayarfbe.1593863

Table1. SASA calculation results of each Cluspro docking simulation.

AMP	TLR	$SASA_{TLR}$ (Å^2)	$SASA_{AMP}$ (Å^2)	$SASA_{COMPLEX}$ (Å^2)	Δ_{SASA} (Å^2)
Betadefensin 1	TLR2	28.267	2.655	28.786	-2.136
Betadefensin 1	TLR3	31.435	2.785	32.037	-2.183
Betadefensin 1	TLR4	28.562	2.730	29.205	-2.087
Betadefensin 1	TLR8	38.059	2.859	37.972	**-2.946**
Betadefensin 1	TLR9	39.121	2.868	38.996	-2.993
Betadefensin 2	TLR2	28.249	4.975	30.130	-3.095
Betadefensin 2	TLR3	31.396	5.051	33.992	-2.455
Betadefensin 2	TLR4	28.693	5.006	30.728	-2.971
Betadefensin 2	TLR8	37.957	5.173	39.139	**-3.991**
Betadefensin 2	TLR9	39.019	5.096	40.299	-3.817
Betadefensin 3	TLR2	28.225	4.005	29.813	-2.418
Betadefensin 3	TLR3	31.360	3.834	32.528	-2.666
Betadefensin 3	TLR4	28.533	3.888	30.310	-2.112
Betadefensin 3	TLR8	37.90	3.899	38.430	-3.373
Betadefensin 3	TLR9	38.934	4.007	39.298	**-3.644**
Betadefensin 4	TLR2	28.319	6.517	31.639	-3.197
Betadefensin 4	TLR3	31.414	6.437	34.303	-3.549
Betadefensin 4	TLR4	28.721	6.587	32.119	-3.189
Betadefensin 4	TLR8	37.849	6.586	39.594	**-4.841**
Betadefensin 4	TLR9	39.049	6.323	41.348	-4.025
CGA-N46	TLR2	28.229	4.558	29.539	-3.249
CGA-N46	TLR3	31.425	4.544	34.127	-1.842
CGA-N46	TLR4	28.661	4.350	30.467	-2.544
CGA-N46	TLR8	37.813	4.535	39.113	-3.234
CGA-N46	TLR9	39.012	4.551	39.739	**-3.824**
Histatin5	TLR2				ND*
Histatin5	TLR3	31.367	2.864	32.595	-1.637
Histatin5	TLR4	28.621	2.872	29.658	-1.836
Histatin5	TLR8	37.934	2.906	37.429	**-3.412**
Histatin5	TLR9	39.047	2.698	38.476	-3.270
LL-37	TLR2				ND*
LL-37	TLR3	31.460	4.207	34.002	-1.666
LL—37	TLR4	28.596	4.107	30.409	-2.296
LL37	TLR8				ND*
LL-37	TLR9	38.952	4.071	39.142	**-3.882**
Psoriasin	TLR2				ND*
Psoriasin	TLR3				ND*
Psoriasin	TLR4	28.619	6.403	31.800	-3.222
Psoriasin	TLR8	37.898	6.140	39.860	**-4.178**

Psoriasin	TLR9	38.950	6.109	41.526	-3.534

*ND: Docking pose unreasonable (i.e. not interacting with the ligand binding interface of the TLR).

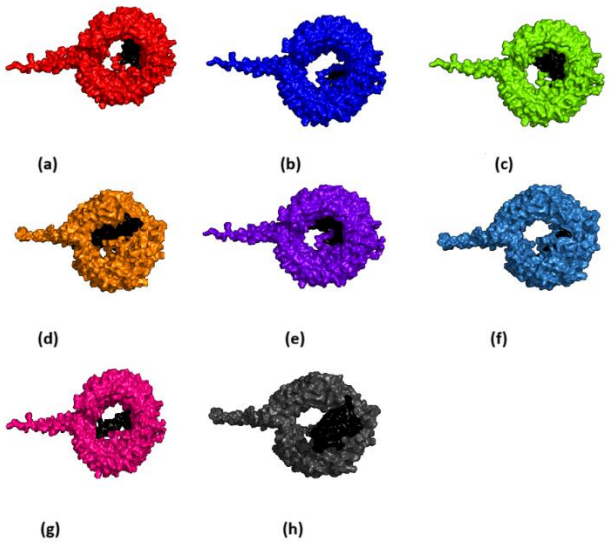

Figure 1. Results with the lowest delta SASA values. Colored structures denote TLRs, black structures denote AMPs (a) Beta defensin 1 - TLR9 (b) Beta defensin 2 - TLR9 (c) Beta defensin 3 - TLR9 (d) Beta defensin 4 - TLR8 (e) CGA-N46 - TLR9 (f) Histatin 5 - TLR8 (g) LL-37 - TLR9 (h) Psoriasin - TLR8.

3.3. Conformational Stabilities of Complexes

MD simulations were next used to probe the stability of the identified docking poses between selected TLRs and AMPs by incorporating the dynamic nature of protein-protein interactions at atomistic scale [40]. Cluspro results yield only rigid interaction information; however, stability of binding is also important for investigation function of AMPs on the body [39]. We thus calculated RMSD-time and RMSF profiles of the complexes subjected to MD simulations (**Figure 2 and Figure 3**).

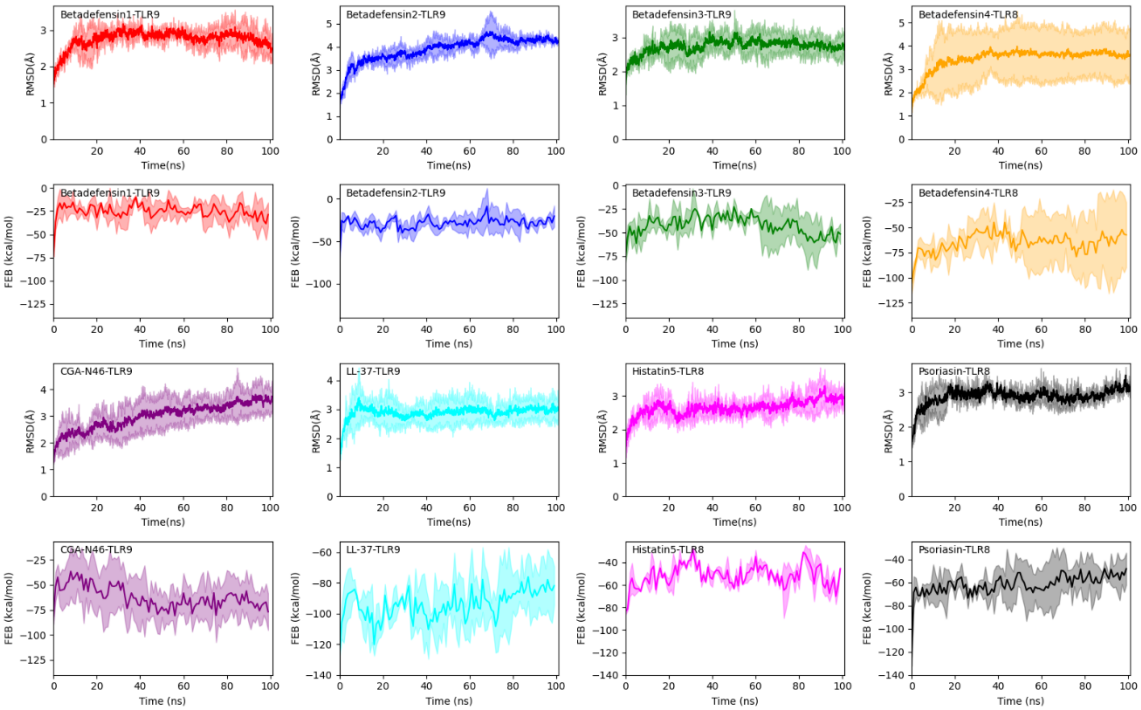

Figure 2. RMSD and FEB time profiles of the simulated TLR-AMP complexes.

Beta defensin 1 - TLR9 complex showed fluctuations between 1.5-3.0 Å in the RMSD plot, whereas beta defensin 2 - TLR9 complex fluctuated around 3.5-4.0 Å. Increased fluctuation at around 60ns of the simulation was identified to be due to changing location of the peptide in the third simulation. After the 80ns, the system appeared to fluctuate around 4 Å with only small deviations. Beta defensin 3 - TLR9 complex was found to fluctuate around 3Å. However, the scale of fluctuations was found to be larger than those involving beta defensin 1 and beta defensin 2. The levels of these fluctuations were found to be even higher for beta defensin 4-TLR8 complex. CGA-N46 – TLR9 simulation could not reach a stable RMS, with a visible drift that lasted until the end of the simulation. LL-37-TLR9 simulation fluctuated around 3 Å until end of the simulation.

In contrast to the RMSD plot, the RMSF profiles were mostly similar to each other, indicating highly stable systems. It should be noted, however, that this does not directly correspond to stability of the bound AMPs to their respective TLR targets. Hence, the RMSD plot was considered a better measure of binding stability of the AMPs.

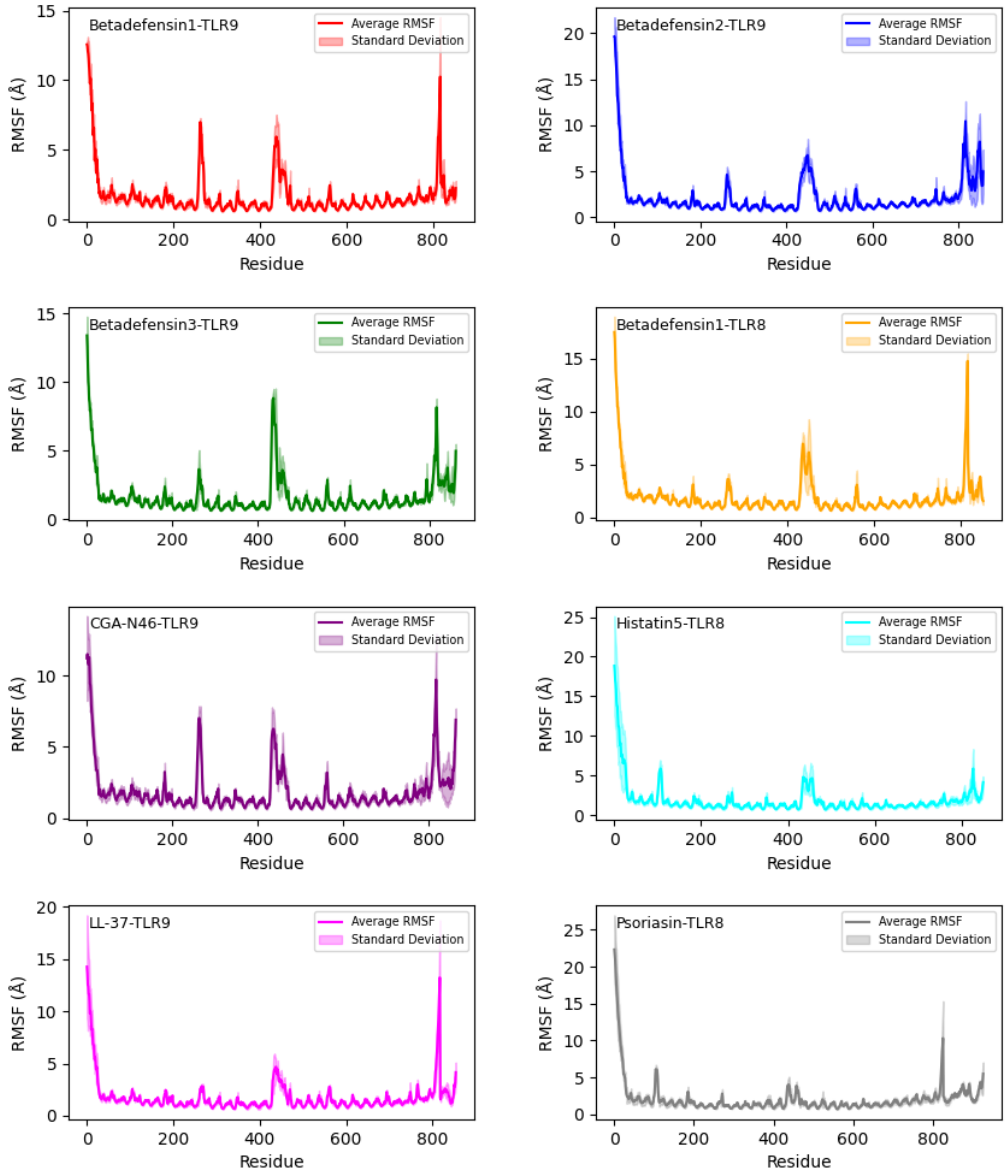

Figure 3. RMSF graphs of TLR-AMP complexes.

FEBs of TLR-AMP complexes as identified during the simulations are also shown in Figure 2 (second and fourth rows). FEB of beta defensin 1-TLR9 and beta defensin 2-TLR9 complexes were found to be similar to each other at around -25 kcal/mol. It is interesting to note that the conformational fluctuation in the beta defensin 2-TLR9 complex at around 60 ns in RMSD plot is also reflected on the FEB time profile, indicating that the conformational change involves a rearrangement of TLR-AMP interaction. The FEB of beta defensin 3-TLR9 interaction was found to deviate around -5 0kcal/mol, and a decreasing profile exists. Beta

defensin4-TLR8 interaction yielded an unstable FEB profile, which deviates between -25 kcal/mol and -50 kcal/mol, again corresponding to the large fluctuation seen in the RMSD plot. CGA-N46-TLR9 complex yielded a decreasing FEB profile from -50 kcal/mol to -75 kcal/mol, indicating that the conformational change observed in the RMSD plot is due to rearrangements of AMP-TLR interactions toward a more stable binding pose. The simulation length was likely not sufficient to identify the final equilibriated interaction mode. LL-37-TLR9 has the lowest average FEB value, which deviated between -80 kcal/mol and -120kcal/mol. Histatin 5-TLR8 and psoriasin-TLR8 complexes also showed similar FEB profiles as in the RMSD plot, and showed deviations between -40 kcal/mol and -80kcal/mol.

Based on empirical findings obtained from murine models, the involvement of TLRs, notably TLR2, TLR4, and TLR9, in *Candida albicans* infections has been indicated. These TLRs primarily induce AMP-responses rather than triggering the production of proinflammatory cytokine [41-43]. Recent interdisciplinary research, integrating experimental observations with computational simulations, has illustrated the multifaceted outcomes resulting from this recognition mechanism. Simultaneously, recent inquiries have emphasized the significant role of TLR-3 in detecting skin injuries by the recognition of damage-associated molecular patterns (DAMPs), which leads to the secretion of cytokines, chemokines, growth factors, and AMPs like LL-37 [44, 45]. While numerous studies have elucidated the impact of AMPs on TLR9 activation through DNA binding, emerging evidence suggests AMPs also modulate TLR3-mediated immune responses to double-stranded RNA (dsRNA). The critical importance of TLR7 and TLR8 has been underscored to clarify their contribution to the host's defence mechanisms against microbial threats [46, 47]. Investigations have delineated TLR8 predominates in monocytes and myeloid dendritic cells (mDCs) to stimulate pro-inflammatory cytokines such as tumor necrosis factor (TNF-α) [48, 49].

4. Conclusions and Outlook

While computer-aided design and high throughput screening methodologies for AMPs have witnessed substantial advancements, a fundamental query persists: are we fostering the development of efficacious therapeutic agents within the immune system? This question presents an intriguing and paradoxical mystery. The enrichment of peptide sequence databases, particularly concerning their relation to TLRs, has significantly contributed to the emergence of peptide-based therapeutic alternatives for Candida infections. However, the current landscape unveils a disjunction between the AMP sequences identified/generated and the functional and structural attributes of TLRs observed in clinical trials, encompassing computationally designed AMPs. Despite the notable progress in peptide-based therapeutic approaches, computationally designed AMPs and their interaction with TLRs have not yet advanced to more sophisticated clinical trials targeting fungal infections. Nonetheless, the substantial advancements in peptide development facilitated by computer-aided methods underscore the potential for enriching AMPs associated with TLRs as future therapeutic options. The pivotal insights provided by these computational approaches, encompassing ClusPro (https://cluspro.org) protein-protein docking server and SASA calculation, hold immense promise for optimizing AMP sequences and their interaction with TLRs, thereby enhancing therapeutic efficacy against Candida infections. Anticipated advancements in highly accurate computational methods are poised to bolster researchers' ability to refine scoring functions for designing and predicting AMP sequences and TLR interactions at a reduced cost. Collectively, these advancements are anticipated to propel computationally designed AMPs and their interaction with TLR agonists and antagonists from database sequences to concrete, effective therapies, with an increased likelihood of reaching the market in the forthcoming years.

Author's Contributions

Mesude Biçer: Conceptualization, Investigation, Writing-original draft, Supervision, Writing-review and editing.

Onur Serçinoğlu: Investigation, Methodology, Data Acquisition, Software

Tuba Okur: Investigation, Methodology, Data Acquisition, Software

Ethics

There are no ethical issues after the publication of this manuscript.

References

[1]. Medici, N. P., Del Poeta, M. 2015. New insights on the development of fungal vaccines: from immunity to recent challenges. *Mem Inst Oswaldo Cruz,* 110, 966-73.

[2]. Bongomin, F., Gago, S., Oladele, R. O., Denning, D. W. 2017. Global and Multi-National Prevalence of Fungal Diseases-Estimate Precision. *J Fungi* (Basel), 3.

[3]. Benedict, K., Richardson, M., Vallabhaneni, S., Jackson, B. R., Chiller, T. 2017. Emerging issues, challenges, and changing epidemiology of fungal disease outbreaks. *Lancet Infect Dis,* 17, e403-e411.

[4]. Quindós, G., Marcos-Arias, C., San-Millán, R., Mateo, E., Eraso, E. 2018. The continuous changes in the aetiology and epidemiology of invasive candidiasis: from familiar Candida albicans to multiresistant Candida auris. *Int Microbiol,* 21, 107-119.

[5]. Robbins, N., Wright, G. D., Cowen, L. E. 2016. Antifungal Drugs: The Current Armamentarium and Development of New Agents. *Microbiol Spectr,* 4.

[6]. Freitas, C. G., Felipe, M. S. 2023. Candida albicans and Antifungal Peptides. *Infectious Diseases and Therapy*, 12, 2631-2648.

[7]. Osset-Trénor, P., Pascual-Ahuir, A., Proft, M. 2023. Fungal Drug Response and Antimicrobial Resistance. *J Fungi (Basel),* 9.

[8]. Pappas, P. G., Kauffman, C. A., Andes, D., Benjamin, D. K. Jr., Calandra, T. F., Edwards, J. E. Jr., Filler, S. G., Fisher, J. F., Kullberg, B. J., Ostrosky-Zeichner, L., Reboli, A. C., Rex, J. H., Walsh, T. J., Sobel, J. D. 2009. Clinical practice guidelines for the management of candidiasis: 2009 update by the Infectious Diseases Society of America. *Clin Infect Dis,* 48, 503-535.

[9]. Barantsevich, N., Barantsevich, E. 2022. Diagnosis and Treatment of Invasive Candidiasis. *Antibiotics (Basel),* 11.

[10]. Andes, D. R., Safdar, N., Baddley, J. W., Playford, G., Reboli, A. C., Rex, J. H., Sobel, J. D., Pappas, P. G., Kullberg, B. J. 2012. Impact of treatment strategy on outcomes in patients with candidemia and other forms of invasive candidiasis: a patient-level quantitative review of randomized trials. *Clin Infect Dis*, 54, 1110-1122.

[11]. Roy, M., Karhana, S., Shamsuzzaman, M., Khan, M. A. 2023. Recent drug development and treatments for fungal infections. *Braz J Microbiol*, 54, 1695-1716.

[12]. Sarkar, S., Uppuluri, P., Pierce, C. G., Lopez-Ribot, J. L. 2014. In vitro study of sequential fluconazole and caspofungin treatment against Candida albicans biofilms. *Antimicrob Agents Chemother*, 58, 1183-1186.

[13]. McKeny, P. T., Nessel, T. A., Zito, P. M. 2024. Antifungal Antibiotics. StatPearls, StatPearls Publishing
Copyright © 2024, StatPearls Publishing LLC., Treasure Island (FL) ineligible companies. Disclosure: Trevor Nessel declares no relevant financial relationships with ineligible companies. Disclosure: Patrick Zito declares no relevant financial relationships with ineligible companies.

[14]. Haney, E. F., Straus, S. K., Hancock, R. E. W. 2019. Reassessing the Host Defense Peptide Landscape. *Frontiers in Chemistry*, 7.

[15]. Haney, E. F., Hancock, R. E. 2013. Peptide design for antimicrobial and immunomodulatory applications. *Biopolymers*, 100, 572-583.

[16]. Nijnik, A., Hancock, R. 2009. Host defence peptides: antimicrobial and immunomodulatory activity and potential applications for tackling antibiotic-resistant infections. *Emerg Health Threats J*, 2, e1.

[17]. Anwar, M. A., Shah, M., Kim, J., Choi, S. 2019. Recent clinical trends in Toll-like receptor targeting therapeutics. *Medicinal Research Reviews*, 39, 1053-1090.

[18]. Baek, M., DiMaio, F., Anishchenko, I., Dauparas, J., Ovchinnikov, S., Lee, G. R., Wang, J., Cong, Q., Kinch, L. N., Schaeffer, R. D., Millán, C., Park, H., Adams, C., Glassman, C. R., DeGiovanni, A., Pereira, J. H., Rodrigues, A. V., van Dijk, A. A., Ebrecht, A. C., Opperman, D. J., Sagmeister, T., Buhlheller, C., Pavkov-Keller T, Rathinaswamy MK, Dalwadi U, Yip CK, Burke JE, Garcia KC, Grishin NV, Adams PD, Read RJ, Baker D. 2021. Accurate prediction of protein structures and interactions using a three-track neural network. *Science*, 373, 871-876.

[19]. Sartorius, R., Trovato, M., Manco, R., D'Apice, L., De Berardinis, P. 2021. Exploiting viral sensing mediated by Toll-like receptors to design innovative vaccines. *npj Vaccines*, 6, 127.

[20]. Murgueitio, M. S., Rakers, C., Frank, A., Wolber, G. 2017. Balancing Inflammation: Computational Design of Small-Molecule Toll-like Receptor Modulators. *Trends in Pharmacological Sciences*, 38, 155-168.

[21]. Billod, J-M., Lacetera, A., Guzmán-Caldentey, J., Martín-Santamaría, S. 2016. Computational Approaches to Toll-Like Receptor 4 Modulation. *Molecules*, 21, 994.

[22]. Jumper, J., Evans, R., Pritzel, A., Green, T., Figurnov, M., Ronneberger, O., Tunyasuvunakool, K., Bates, R., Žídek, A., Potapenko, A., Bridgland, A., Meyer, C., Kohl, S. A. A., Ballard, A. J., Cowie, A., Romera-Paredes, B., Nikolov, S., Jain, R., Adler, J., Back, T., Petersen, S., Reiman, D., Clancy, E., Zielinski, M., Steinegger, M., Pacholska, M., Berghammer, T., Bodenstein, S., Silver, D., Vinyals, O., Senior, A. W., Kavukcuoglu, K., Kohli, P., Hassabis, D. 2021. Highly accurate protein structure prediction with AlphaFold. *Nature*, 596, 583-589.

[23]. Burley, S. K., Bhikadiya, C., Bi, C., Bittrich, S., Chao, H., Chen, L., Craig, P. A., Crichlow, G. V., Dalenberg, K., Duarte, J. M., Dutta, S., Fayazi, M., Feng, Z., Flatt, J. W., Ganesan, S., Ghosh, S., Goodsell, D. S., Green, R. K., Guranovic, V., Henry, J., Hudson, B. P., Khokhriakov, I., Lawson, C. L., Liang, Y., Lowe, R., Peisach, E., Persikova, I., Piehl, D. W., Rose, Y., Sali, A., Segura, J., Sekharan, M., Shao, C., Vallat, B., Voigt, M., Webb, B., Westbrook, J. D., Whetstone, S., Young, J. Y., Zalevsky, A., Zardecki, C. 2022. RCSB Protein Data Bank (RCSB.org): delivery of experimentally-determined PDB structures alongside one million computed structure models of proteins from artificial intelligence/machine learning. *Nucleic Acids Research*, 51, D488-D508.

[24]. Mirdita, M., Schütze, K., Moriwaki, Y., Heo, L., Ovchinnikov, S., Steinegger, M. 2022. ColabFold: making protein folding accessible to all. *Nature Methods*, 19, 679-682.

[25]. Kozakov, D., Hall, D. R., Xia, B., Porter, K. A., Padhorny, D., Yueh, C., Beglov, D., Vajda, S. 2017. The ClusPro web server for protein–protein docking. *Nature Protocols*, 12, 255-278.

[26]. Jo, S., Kim, T., Iyer, V. G., Im, W. 2008. CHARMM-GUI: A web-based graphical user interface for CHARMM. *Journal of Computational Chemistry*, 29, 1859-1865.

[27]. Lee, J., Cheng, X., Swails, J. M., Yeom, M. S., Eastman, P. K., Lemkul, J. A., Wei, S., Buckner, J., Jeong, J. C., Qi, Y., Jo, S., Pande, V. S., Case, D. A., Brooks, C. L., 3rd, MacKerell, A. D., Klauda, J. B., Im, W. 2016. CHARMM-GUI Input Generator for NAMD, GROMACS, AMBER, OpenMM, and CHARMM/OpenMM Simulations Using the CHARMM36 Additive Force Field. *J Chem Theory Comput*, 12, 405-413.

[28]. Huang, J., Rauscher, S., Nawrocki, G., Ran, T., Feig, M., de Groot, B. L., Grubmüller, H., MacKerell, A. D. 2017. CHARMM36m: an improved force field for folded and intrinsically disordered proteins. *Nature Methods*, 14, 71-73.

[29]. Abraham, M. J., Murtola, T., Schulz, R., Páll, S., Smith, J. C., Hess, B., Lindahl, E. 2015. GROMACS: High performance molecular simulations through multi-level parallelism from laptops to supercomputers. *SoftwareX*, 1(2):19-25.

[30]. Humphrey, W., Dalke, A., Schulten, K. 1996. VMD: Visual molecular dynamics. *Journal of Molecular Graphics*, 14, 33-38.

[31]. Bakan, A., Meireles, L. M., Bahar, I. 2011. ProDy: Protein Dynamics Inferred from Theory and Experiments. *Bioinformatics*, 27, 1575-1577.

[32]. Miller, B. R. III., McGee, T. D., Swails, J. M., Homeyer, N., Gohlke, H., Roitberg, A. E. 2012. MMPBSA.py: An Efficient Program for End-State Free Energy Calculations. *Journal of Chemical Theory and Computation*, 8, 3314-3321.

[33]. Valdés-Tresanco, M. S, Valdés-Tresanco, M. E., Valiente, P. A., Moreno, E. 2021. gmx_MMPBSA: A New Tool to Perform End-State Free Energy Calculations with GROMACS. *J Chem Theory Comput*, 17, 6281-6291.

[34]. Sameer, A. S., Nissar, S. 2021. Toll-Like Receptors (TLRs): Structure, Functions, Signaling, and Role of Their Polymorphisms in Colorectal Cancer Susceptibility. *Biomed Res Int*, 2021, 1157023.

[35]. Lee EY, Lee MW, Wong GCL (2019) Modulation of toll-like receptor signaling by antimicrobial peptides. Semin Cell Dev Biol 88:173-184.

[36]. Kumar, N., Sood, D., Tomar, R., Chandra, R. 2019. Antimicrobial Peptide Designing and Optimization Employing Large-Scale Flexibility Analysis of Protein-Peptide Fragments. *ACS Omega*, 4, 21370-21380.

[37]. Zhang, Y., Liang, X., Bao, X., Xiao, W., Chen, G. 2022. Toll-like receptor 4 (TLR4) inhibitors: Current research and prospective. *European Journal of Medicinal Chemistry*, 235, 114291.

[38]. Konstantinidis, K., Karakasiliotis, I., Anagnostopoulos, K., Boulougouris, G. C. 2021. On the estimation of the molecular inaccessible volume and the molecular accessible surface of a ligand in protein–ligand systems. *Molecular Systems Design & Engineering*, 6, 946-963.

[39]. Chaieb, K., Kouidhi, B., Hosawi, S. B., Baothman, O. A. S., Zamzami, M. A., Altayeb, H. N. 2022. Computational screening of natural compounds as putative quorum sensing inhibitors targeting drug resistance bacteria: Molecular docking and molecular dynamics simulations. *Computers in Biology and Medicine*, 145, 105517.

[40]. Agarwal, S. M., Nandekar, P., Saini, R. 2022. Computational identification of natural product inhibitors against EGFR double mutant (T790M/L858R) by integrating ADMET, machine learning, molecular docking and a dynamics approach. *RSC Advances,* 12, 16779-16789.

[41]. Bellocchio, S., Gaziano, R., Bozza, S., Rossi, G., Montagnoli, C., Perruccio, K., Calvitti, M., Pitzurra, L., Romani, L. 2005. Liposomal amphotericin B activates antifungal resistance with reduced toxicity by diverting Toll-like receptor signalling from TLR-2 to TLR-4. *J Antimicrob Chemother*, 55, 214-222.

[42]. van de Veerdonk, F. L., Netea, M. G., Jansen, T. J., Jacobs, L., Verschueren, I., van der Meer, J. W., Kullberg, B. J. 2008. Redundant role of TLR9 for anti-Candida host defense. *Immunobiology*, 213, 613-620.

[43]. Naglik, J. R., Richardson, J. P., Moyes, D. L. 2014. Candida albicans pathogenicity and epithelial immunity. *PLoS Pathog*, 10, e1004257.

[44]. Adase, C. A., Borkowski, A. W., Zhang, L. J., Williams, M. R., Sato, E., Sanford, J. A., Gallo, R. L. 2016. Non-coding Double-stranded RNA and Antimicrobial Peptide LL-37 Induce Growth Factor Expression from Keratinocytes and Endothelial Cells. *J Biol Chem*, 291, 11635-11646.

[45]. Zhang, L. J., Sen, G. L., Ward, N. L., Johnston, A., Chun, K., Chen, Y., Adase, C., Sanford, J. A., Gao, N., Chensee, M., Sato, E., Fritz, Y., Baliwag, J., Williams, M. R., Hata, T., Gallo, R. L. 2016. Antimicrobial Peptide LL37 and MAVS Signaling Drive Interferon-β Production by Epidermal Keratinocytes during Skin Injury. *Immunity*, 45,119-130.

[46]. Heil, F., Hemmi, H., Hochrein, H., Ampenberger, F., Kirschning, C., Akira, S., Lipford, G., Wagner, H., Bauer, S. 2004. Species-specific recognition of single-stranded RNA via toll-like receptor 7 and 8. *Science*, 303, 1526-1529.

[47]. Lund, J. M., Alexopoulou, L., Sato, A., Karow, M., Adams, N. C., Gale, N. W., Iwasaki, A., Flavell, R. A. 2004. Recognition of single-stranded RNA viruses by Toll-like receptor 7. *Proc Natl Acad Sci U S A*, 101, 5598-5603.

[48]. Sun, H., Li, Y., Zhang, P., Xing, H., Zhao, S., Song, Y., Wan, D., Yu, J. 2022. Targeting toll-like receptor 7/8 for immunotherapy: recent advances and prospectives. *Biomarker Research,* 10, 89.

[49]. Hanten, J. A., Vasilakos, J. P., Riter, C. L., Neys, L., Lipson, K. E., Alkan, S. S., Birmachu, W. 2008. Comparison of human B cell activation by TLR7 and TLR9 agonists. *BMC Immunol*, 9, 39.